IOP PUBLISHING PHYSICS IN MEDICINE AND BIOLOGY

Phys. Med. Biol. **53** (2008) 4093–4106 doi:10.1088/0031-9155/53/15/006

HDRK-Man: a whole-body voxel model based on high-resolution color slice images of a Korean adult male cadaver

Chan Hyeong Kim[1], **Sang Hyoun Choi**[2], **Jong Hwi Jeong**[1], **Choonsik Lee**[3] **and Min Suk Chung**[4]

[1] Department of Nuclear Engineering, Hanyang University, 17 Haengdang-dong, Seongdong-gu, Seoul 133-791, Korea
[2] Department of radiation oncology, Inha University, 7-206, 3-ga, Shinheumg-dong, Jung-gu, Incheon, 400-711, Korea
[3] Department of Nuclear and Radiological Engineering, University of Florida, Gainesville, FL 32611, USA
[4] Department of Anatomy, Ajou University School of Medicine, San 5 Wonchon-dong, Yeongtong-gu, Suwon 443-749, Korea

E-mail: chkim@hanyang.ac.kr

Received 31 March 2008, in final form 30 May 2008
Published 8 July 2008
Online at stacks.iop.org/PMB/53/4093

Abstract

A Korean voxel model, named 'High-Definition Reference Korean-Man (HDRK-Man)', was constructed using high-resolution color photographic images that were obtained by serially sectioning the cadaver of a 33-year-old Korean adult male. The body height and weight, the skeletal mass and the dimensions of the individual organs and tissues were adjusted to the reference Korean data. The resulting model was then implemented into a Monte Carlo particle transport code, MCNPX, to calculate the dose conversion coefficients for the internal organs and tissues. The calculated values, overall, were reasonable in comparison with the values from other adult voxel models. HDRK-Man showed higher dose conversion coefficients than other models, due to the facts that HDRK-Man has a smaller torso and that the arms of HDRK-Man are shifted backward. The developed model is believed to adequately represent average Korean radiation workers and thus can be used for more accurate calculation of dose conversion coefficients for Korean radiation workers in the future.

(Some figures in this article are in colour only in the electronic version)

1. Introduction

The voxel model, also called the 'tomographic model', first reported by Gibbs *et al* (1984), was used to calculate effective doses for dental radiology examinations. The first model was

the representation of the head and torso from computed tomography (CT) of a female cadaver. Zubal *et al* (1994) constructed an adult male model from the CT data of an adult male patient of dimensions similar to the Reference Man data in ICRP 23 (ICRP 1975). Dimbylow (1996) constructed an adult male model called NORMAN from the whole-body magnetic resonance (MR) images of a healthy volunteer. The voxel resolution was scaled in order to match the height and weight of the segmented model to the ICRP 23 reference data (ICRP 1975). More recently, Zankl *et al* (2005) and Schlattl *et al* (2007) adjusted the dimensions of the previously constructed adult male and female models, Golem and Laura, to the reference values in ICRP 89 (ICRP 2002) and 70 (ICRP 1994). The adjustment was fairly comprehensive, including the body height and weight, the skeletal mass and the dimensions of individual organs and tissues. The developed models, which were named 'Rex' and 'Regina', have been adopted by the ICRP as reference phantoms for the forthcoming updates of the dose conversion coefficients for workers and adult members of the public (Schlattl *et al* 2007).

Acknowledging the anatomical and physical differences between the different racial groups, Saito *et al* (2001) constructed a Japanese voxel model Otoko by segmenting the whole-body CT images of a patient whose external dimensions were in good agreement with the Japanese Reference Man data (Tanaka *et al* 1989). Meanwhile, several Korean voxel models were also constructed in Korea, by Lee and Lee (2006), using MR and CT images. The KTMAN-2 model, the most recent model, was constructed using the CT images of a 35-year-old healthy adult male volunteer. The volunteer had a height and weight of 172 cm and 68 kg, respectively, which are close to the Reference Korean data for male (171 cm, 68 kg) (Park *et al* 2006b). The developed model is 172 cm in height and 66.8 kg in weight, having a voxel resolution of 2 mm $\times$ 2 mm $\times$ 5 mm.

In general, CT and MR images provide fairly good information for accurate delineation of organs, but it is difficult to delineate some organs accurately if they are of similar material composition (e.g. ovaries, pancreas, esophagus, adrenals and thymus) or in continuous movement (e.g. gastro-intestines and heart) (Caon 2004). Consequently, the segmentation process involves significant subjective decisions that can impair the integrity of the resulting model. In fact, it has been reported that 'the uncertainties associated with organ masses will be (of the) order of 10% or more' (Caon 2004). Xu *et al* (2000) constructed a high-resolution voxel model, called VIP-Man, based on color photographic slice images of a cadaver of a 38-year-old male. VIP-Man, which has the voxel resolution of 0.33 mm $\times$ 0.33 mm $\times$ 1 mm, is known to be the most complete body description so far. The model, however, is of only limited value for use in radiation protection, in that it represents a relatively large person (186 cm in height and 103 kg in weight), which is a significant deviation from the ICRP reference data (176 cm and 73 kg) and even more of a deviation from the Reference Korean data (171 cm and 68 kg).

Recently, the Visible Korean Human (VKH) was initiated in Korea (Chung *et al* 2002), in which photographic slice images were obtained from the cadaver of a 33-year-old Korean male (164 cm in height and 55 kg in weight). The skeleton, lungs, liver, brain, kidneys, skin (external surface), urinary bladder (external surface), heart (internal surface), gastro-intestinal tract (internal surface), main arteries (internal surface) and respiratory tract (internal surface) were segmented by professional anatomists (Park *et al* 2006a).

This paper describes the construction of a high-quality Korean voxel model, named 'High-Definition Reference Korean-Man (HDRK-Man)', which was constructed using high-resolution color photographic slice images. The present study was built upon the previous work (Park *et al* 2006a); that is, the present work adopted the organs that had already been segmented in the previous study. The present study segmented the organs and tissues that were not segmented, or were partly segmented, in the previous work. The dimensions,

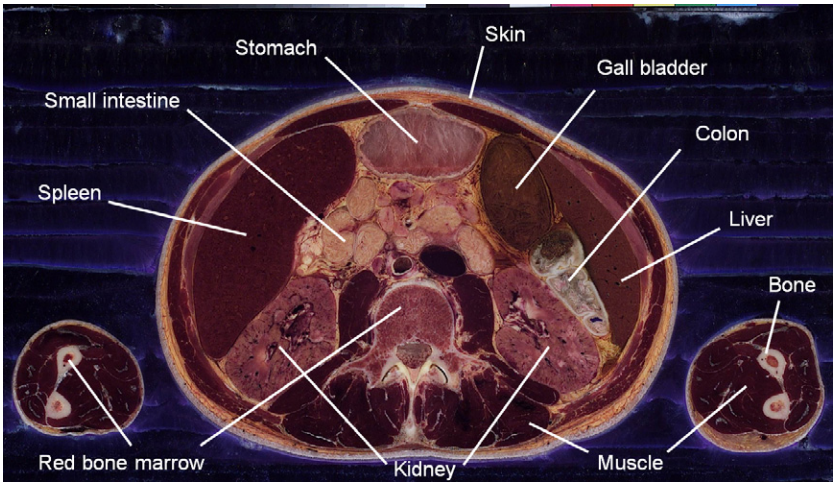

Figure 1. Example of color photographic slice image at abdomen, utilized in model construction.

including the body height and weight, the skeletal mass and those of the individual organs and tissues, were adjusted to the reference Korean data (Park *et al* 2006b) according to the procedure followed in the construction of the ICRP reference phantoms, Rex and Regina (Schlattl *et al* 2007). The model was implemented into a general purpose Monte Carlo particle transport code, MCNPX (Pelowitz 2005), to calculate the dose conversion coefficients for four idealized photon irradiation geometries: antero-posterior (AP), postero-anterior (PA), right-lateral (RLAT), and left-lateral (LLAT). The results were then compared with the reported values from other computational models, that is, one Korean voxel model, KTMAN-2, and two Caucasian-based voxel models, Rex and VIP-Man.

2. Materials and methods

2.1. VKH anatomical images

HDRK-Man was developed using the color photographic slice images (figure 1) from the VKH project (Chung *et al* 2002). The images were obtained from the cadaver of a 33-year-old Korean male (164 cm in height and 55 kg in weight) who had died of leukemia. The cadaver was fixed, embedded and frozen in an immobilization box. It was then serially sectioned transverse to the longitudinal direction at 0.2 mm intervals with a cryomacrotome, and each sectioned surface was photographed with a Kodak DSC560 digital camera providing 3040 $\times$ 2008 pixel resolution (Kodak, Rochester, NY). The images were saved in Tag Image File Format (TIFF) (24 bit color). A total of 8590 photographic images of 0.1875 mm $\times$ 0.1875 mm resolution were acquired from the cadaver. The color quality and high resolution of the slice images made it possible to accurately segment the organs and tissues, especially the small anatomical structures. The researchers also acquired CT and MR images at 1 mm intervals for possible future use. The skeleton, lungs, liver, brain, kidneys, skin (external surface), urinary bladder (external surface), heart (internal surface), gastro-intestinal tract (internal surface), main arteries (internal surface) and respiratory tract (internal surface) were segmented by professional anatomists (Park *et al* 2006a).

2.2. Segmentation of organs

The color photographic images used in the present study were better for segmentation purposes than gray-scale CT or MR images mainly because the colors in the photographic images made different tissues distinguishable, whereas they would have been less distinguishable in the gray-scale CT or MR images. The present study was built upon the previous work (Park *et al* 2006a); that is, the present work adopted the organs that had already been segmented in the previous study. The present study segmented the organs and tissues that were not segmented in the previous work as well as the organs that had been only partly segmented in the previous study (i.e. urinary bladder (for internal surface), heart (for external surface) and gastro-intestinal tract (for external surface). Color anatomical images for model construction were selected at every 2 mm interval; that is, 850 images were selected out of the total of 8590 images. The organs and tissues, clearly distinguished by color, were segmented automatically using Photoshop 7.0 (Abode Systems, Inc., San Jose, CA) and Interactive Data Language (IDL) 5.6. The automatic process was used for the eyes, lenses, skeleton, skin, muscle, colon, small intestine, extrathoracic (ET) region, red bone marrow and gall bladder. The other organs, those that could not be segmented automatically, were segmented manually using a screen digitizer CINTIQ 15X (WACOM Co., Ltd, Japan) and the magnetic lasso tool in Photoshop 7.0. The magnetic lasso tool, which automatically marks the region of selection by identifying differences of color, significantly expedited the segmentation process. The thyroid, urinary bladder, prostate, salivary glands, adrenals, esophagus, spleen, stomach, lungs, brain, liver, thymus, pancreas, gonads, kidneys, heart, oral mucosa and blood were segmented manually. The skeleton was divided into nine bone regions, that is, skull, mandible, ribcage, pelvis, spine, upper arm bone, lower arm bone, upper leg bone and lower leg bone (Kramer *et al* 2003, ICRP 1994), and the red bone marrow (RBM) was segmented considering the distribution of RBM in those regions. Because the RBM cavities are very small ($<10\ \mu$m), the distribution of the RBM in each bone region was not determined microscopically, but determined macroscopically following the approach used in a previous study (Chao 2001). The color of each pixel in a bone region was measured, and the redness of the pixel was used to determine if the pixel is a RBM pixel or not. The only difference is that, in the present study, the RBM was segmented considering the distribution of the RBM in different bone regions. After completing the segmentation, the resolution of the segmented images was reduced to 1.875 mm $\times$ 1.875 mm for compatibility with the computation speed and memory size of the computers in use, resulting in an intermediate voxel resolution of 1.875 mm $\times$ 1.875 mm $\times$ 2 mm.

2.3. Adjustment of height and skeletal mass

The body height of the voxel model was adjusted by changing the voxel resolution; that is, the height (164 cm) was matched to the height of the reference Korean (171 cm) by adjusting the z-resolution from 2 to 2.0854 mm. The total skeletal mass was not available in the reference Korean data, and therefore, it was estimated by the method suggested by Clays *et al* (ICRP 1994):

$$m = -10.7 + 0.119 \times HT \quad \text{(kg)} \tag{1}$$

where m is the skeletal mass in kg and HT is the height in cm. The height of the reference Korean is 171 cm, and thus the skeletal mass was calculated as 9.6 kg. The original skeletal mass of 8.6 kg was then matched to 9.6 kg (including RBM) by increasing the in-plane voxel size from 1.875 mm $\times$ 1.875 mm to 1.981 mm $\times$ 1.981 mm. Consequently, the voxel resolution of the final model was 1.981 mm $\times$ 1.981 mm $\times$ 2.0854 mm.

Figure 2. Deformation of spleen due to adjustment (left: before adjustment and right: after adjustment).

2.4. Adjustment of individual organs and body weight

The dimensions of the individual organs were adjusted to the reference Korean data (partially to the reference Asian data, in the cases of organs and tissues for which reference Korean data were not available) by utilizing the inner grow and outer grow functions in Photoshop 7.0. The organs that were larger than those in the reference Korean data were adjusted by erosion (inner grow), and the eroded regions were filled with adipose tissue. The organs smaller than those of the reference Korean were adjusted by dilation (outer grow), adding pixels onto the organ surfaces. The remaining volume in the model, including all of the undefined organs and tissues, was defined as adipose tissue.

The volunteer died of leukemia, and the spleen was several times larger than that of an average person. The adjustment of the spleen was therefore considered unrealistic, significantly deforming the external shape of the organ. Nevertheless, the spleen was adjusted to the reference Korean data to keep consistency with the other organs in the model. Figure 2 shows the unwanted deformation of the spleen due to the adjustment.

On completion of the adjustments for the body height, skeletal mass and organ dimensions, the weight of the model was 67.8 kg, which was less than the weight of the reference Korean (68 kg) by only 0.2 kg. The weight was then adjusted simply by adding 0.2 kg of adipose tissue to the lower parts of the legs. The average tissue compositions and densities in ICRU 46 (ICRU 1992) were used to describe the tissues, except for the lungs and skeleton. The lung density (0.296 g cm^{-3}) and composition were taken from ICRP 23 (ICRP 1975). The skeletal density (1.34 g cm^{-3}) and composition were recalculated from the reference values in ICRP 70 (ICRP 1994) and ICRP 23, respectively, subtracting the elemental composition of RBM, which was explicitly segmented in the present study, from the homogeneous skeletal composition.

2.5. Monte Carlo organ dose calculations

The developed model, HDRK-Man, was implemented into the Monte Carlo particle transport code MCNPX (Pelowitz 2005) for the calculation of the organ-absorbed doses. The three-dimensional (3D) array of the voxel model was converted into a format that could be handled by MCNPX, and the resulting size of the MCNPX input file was about 94 megabytes. The energy deposition tally of track-length estimation, F6, was used to calculate the organ doses. The F6 tally essentially calculates organ-averaged collision kerma in MeV g^{-1} per source particle, which was then approximated as an organ-averaged absorbed dose, or organ dose, assuming charged particle equilibrium in all of the organs and tissues of HDRK-Man. The number of source photons transported in the Monte Carlo simulations were 10^8 for 0.015 MeV,

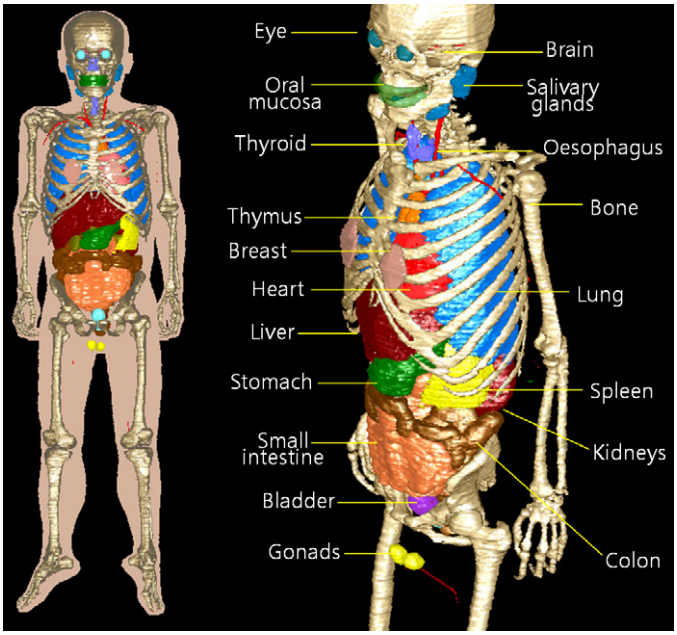

Figure 3. 3D whole-body frontal view with semi-transparent skin (left) and major organs and tissues (right) of HDRK-Man.

3×10^7 for 0.03–0.05 MeV and 10^7 for the higher energies. The computation time for each case was 50–260 min on a HP ProLiant ML570G3 machine equipped with a 3.0 GHz Intel Xeon^{TM} processor and 1024 MB RAM. The statistical errors in the organ doses were less than 5%, except for 0.015 MeV, for which the statistical errors were as large as 100%.

3. Results and discussion

3.1. HDRK-Man

The adult Korean male voxel model, HDRK-Man, was constructed from high-resolution photographic anatomical images to represent average Korean radiation workers. Figure 3 shows 3D views of the major organs and tissues. The voxel model is 171 cm in height and 68 kg in weight. The size of the voxels (voxel resolution) is $1.981 \times 1.981 \times 2.0854$ mm^3, and the voxel array size is $247 \times 141 \times 850$ (29 602 950) in the x, y and z directions, which correspond to 489.307, 279.321 and 1772.59 mm, respectively. The model includes a total of 30 organs and tissues that are required to calculate an effective dose.

Table 1 shows the organ and tissue masses of HDRK-Man along with the reference values used for adjustment. The reference Asian data (IAEA 1998) were used for the prostate, bladder, adrenals, colon and small intestines, for which reference Korean data were not available. The organ masses are in overall good agreement with the reference Korean data, specifically within 7%, except for the following organs and tissue: the eye lenses were not adjusted due to the limitation of the voxel resolution; the thickness of skin is known to be 1.47–2.45 mm (ICRP 2002), but, in the present study, the skin was represented simply by one layer of voxels on the surface of the body; the adipose tissue of HDRK-Man is much heavier than the reference

Table 1. HDRK-Man organ and tissue masses.

	Mass (g)		
Organ	HDRK-Man	reference Korean	Difference (%)
Bone	9607	9649	−0.4
Liver	1474	1438	2.5
Lungs	1156	1123	2.9
Brain	1620	1522	6.4
Kidneys	359	338	6.2
Spleen	177	170	4.1
Stomach	141	140	0.7
Pancreas	126	130	−3.1
Thymus	39	40	−2.5
Gonads	28	29	−3.4
Eyes	21	20	5.0
Lens	0.51	0.4	27.5
Muscle	23 300	25 000	−6.8
Bladder	42	40[a]	5.0
Colon	343	330[a]	3.9
Small intestine	602	590[a]	2.0
Esophagus	40	40	0.0
Adrenals	14	14[a]	0.0
Skin	4260	2400	77.5
Extrathoracic region	73	–	–
Thyroid	15	15	0.0
Bone marrow (red)	1068	1000	6.8
Prostate	12	12[a]	0.0
Blood	254	–	–
Salivary glands	87	82	6.1
Gall bladder	13	13	0.0
Oral mucosa	21	–	–
Heart wall	391	380	2.9
Breast	23.3	22	5.9
Adipose tissue	23 400.2	11 000	112.7

[a] The reference Asian data were used for the organs and tissues for which reference Korean data were not available.

Korean data, because not only the adipose tissue itself but also all of the undefined organs were defined as adipose tissue.

3.2. Dose conversion coefficients

The dose conversion coefficients, which were organ-averaged absorbed doses per unit air kerma free-in-air (D_T/K_a), calculated by HDRK-Man, were compared with the reported values from other models, KTMAN-2 (Lee and Kim 2004), Rex (Schlattl *et al* 2007) and VIP-Man (Chao 2001). Four idealized irradiation geometries were compared: antero-posterior (AP), postero-anterior (PA), left-lateral (LLAT) and right-lateral (RLAT). Table 2 shows the dose-conversion coefficients calculated with MCNPX coupled with HDRK-Man. In general, the calculated values were very reasonable when compared with the values from other models; see figure 4 for an example.

Table 2. Dose conversion coefficients calculated from HDRK-Man.

Energy (MeV)	AP	PA	RLAT	LLAT	AP	PA	RLAT	LLAT	AP	PA	RLAT	LLAT
		Bladder				Bone marrow (red)				Bone		
0.015	0.002	–	–	–	0.003	0.003	0.002	0.002	0.032	0.016	0.016	0.016
0.030	0.369	0.091	0.017	0.019	0.131	0.182	0.066	0.067	0.866	0.691	0.484	0.488
0.040	0.817	0.319	0.087	0.100	0.339	0.466	0.176	0.177	1.822	1.598	1.029	1.030
0.050	1.189	0.573	0.202	0.225	0.570	0.759	0.303	0.304	2.511	2.295	1.445	1.440
0.080	1.527	0.911	0.416	0.448	0.911	1.156	0.512	0.512	2.457	2.335	1.457	1.454
0.200	1.228	0.854	0.447	0.485	0.880	1.070	0.534	0.535	1.195	1.148	0.755	0.754
0.400	1.093	0.845	0.511	0.538	0.851	0.996	0.557	0.555	0.993	0.956	0.668	0.667
0.600	1.057	0.824	0.550	0.583	0.851	0.974	0.583	0.582	0.955	0.924	0.670	0.668
0.800	1.040	0.842	0.582	0.631	0.861	0.968	0.611	0.610	0.947	0.919	0.684	0.683
2.000	1.006	0.898	0.723	0.736	0.896	0.970	0.712	0.711	0.948	0.930	0.756	0.755
8.000	0.999	0.935	0.843	0.852	0.929	0.971	0.818	0.818	0.994	0.982	0.874	0.873
10.000	0.996	0.934	0.846	0.854	0.930	0.969	0.825	0.824	1.004	0.993	0.890	0.889
		Brain				Breast				Colon		
0.015	–	–	–	–	0.410	–	0.050	0.038	0.014	–	0.001	0.001
0.030	0.127	0.136	0.159	0.154	0.806	0.008	0.300	0.253	0.431	0.155	0.172	0.142
0.040	0.381	0.417	0.450	0.440	1.015	0.045	0.425	0.368	0.853	0.424	0.372	0.329
0.050	0.630	0.682	0.719	0.701	1.233	0.104	0.550	0.485	1.191	0.697	0.550	0.499
0.080	0.903	0.947	0.984	0.972	1.577	0.251	0.789	0.705	1.482	1.033	0.741	0.696
0.200	0.813	0.843	0.870	0.862	1.481	0.394	0.897	0.808	1.177	0.909	0.672	0.637
0.400	0.801	0.826	0.850	0.842	1.339	0.494	0.918	0.842	1.061	0.864	0.677	0.643
0.600	0.815	0.837	0.857	0.850	1.276	0.564	0.928	0.861	1.028	0.860	0.698	0.667
0.800	0.829	0.851	0.868	0.865	1.245	0.616	0.940	0.879	1.013	0.865	0.719	0.692
2.000	0.891	0.904	0.915	0.912	1.177	0.765	0.986	0.947	0.997	0.898	0.798	0.782
8.000	0.938	0.943	0.949	0.948	1.092	0.852	0.982	0.960	0.989	0.926	0.877	0.865
10.000	0.939	0.943	0.949	0.948	1.077	0.848	0.974	0.951	0.985	0.926	0.880	0.868
		Gonads				Liver				Lungs		
0.015	0.123	0.009	0.005	–	0.004	–	–	–	0.001	0.001	0.001	0.001
0.030	1.022	0.156	0.094	0.053	0.338	0.067	0.169	0.041	0.238	0.267	0.156	0.120
0.040	1.462	0.363	0.209	0.158	0.795	0.258	0.464	0.156	0.595	0.654	0.363	0.286
0.050	1.749	0.551	0.318	0.268	1.192	0.491	0.746	0.295	0.910	0.991	0.553	0.447
0.080	1.835	0.787	0.458	0.410	1.550	0.814	1.027	0.488	1.221	1.322	0.755	0.631
0.200	1.431	0.722	0.490	0.443	1.175	0.722	0.867	0.475	1.000	1.099	0.667	0.573
0.400	1.248	0.782	0.549	0.506	1.044	0.715	0.833	0.511	0.934	1.021	0.669	0.589
0.600	1.190	0.802	0.598	0.561	1.007	0.730	0.837	0.548	0.923	0.999	0.690	0.620
0.800	1.159	0.818	0.634	0.595	0.995	0.751	0.848	0.583	0.925	0.994	0.716	0.650
2.000	1.091	0.887	0.751	0.730	0.982	0.820	0.895	0.704	0.946	0.994	0.802	0.755
8.000	1.048	0.923	0.847	0.843	0.981	0.881	0.936	0.821	0.965	0.989	0.882	0.855
10.000	1.043	0.921	0.855	0.852	0.979	0.882	0.935	0.828	0.964	0.986	0.887	0.860
		Esophagus				Salivary glands				Skin		
0.015	–	–	–	–	0.006	0.008	0.049	0.059	0.373	0.359	0.218	0.217
0.030	0.135	0.066	0.043	0.062	0.272	0.311	0.393	0.440	0.700	0.675	0.448	0.447
0.040	0.434	0.316	0.176	0.237	0.552	0.577	0.630	0.687	0.876	0.850	0.570	0.570
0.050	0.752	0.619	0.352	0.434	0.794	0.798	0.826	0.888	1.012	0.985	0.664	0.664
0.080	1.161	1.060	0.587	0.705	1.059	1.048	1.025	1.103	1.139	1.109	0.763	0.763
0.200	0.936	0.899	0.603	0.661	0.989	1.001	0.937	0.979	1.044	1.016	0.744	0.744
0.400	0.883	0.848	0.627	0.682	0.965	0.982	0.901	0.938	1.004	0.979	0.752	0.753
0.600	0.877	0.841	0.661	0.714	0.953	0.982	0.898	0.929	0.995	0.972	0.769	0.770
0.800	0.877	0.845	0.699	0.736	0.959	0.985	0.903	0.935	0.995	0.974	0.786	0.788
2.000	0.900	0.886	0.804	0.828	0.985	1.003	0.935	0.952	1.001	0.986	0.848	0.850
8.000	0.923	0.912	0.872	0.887	0.984	0.985	0.951	0.956	0.995	0.987	0.906	0.909
10.000	0.924	0.912	0.873	0.888	0.978	0.980	0.951	0.955	0.992	0.984	0.908	0.911

Table 2. (Continued.)

Energy (MeV)	AP	PA	RLAT	LLAT	AP	PA	RLAT	LLAT	AP	PA	RLAT	LLAT
		Stomach				Thyroid				Adrenals		
0.015	0.020	–	–	–	0.061	–	0.001	–	–	–	–	–
0.030	0.538	0.032	0.073	0.161	0.918	0.028	0.191	0.158	0.084	0.124	0.020	0.033
0.040	1.005	0.168	0.210	0.443	1.505	0.179	0.483	0.427	0.318	0.436	0.112	0.149
0.050	1.378	0.359	0.351	0.694	1.907	0.426	0.742	0.682	0.595	0.781	0.256	0.306
0.080	1.699	0.671	0.543	0.961	2.134	0.731	0.975	0.953	0.996	1.228	0.474	0.531
0.200	1.284	0.638	0.544	0.843	1.539	0.669	0.832	0.817	0.888	1.059	0.499	0.538
0.400	1.144	0.648	0.582	0.837	1.327	0.677	0.833	0.823	0.846	0.988	0.519	0.571
0.600	1.095	0.676	0.618	0.850	1.250	0.696	0.857	0.849	0.846	0.954	0.544	0.584
0.800	1.074	0.702	0.654	0.866	1.221	0.719	0.881	0.876	0.863	0.948	0.576	0.612
2.000	1.041	0.782	0.767	0.917	1.146	0.822	0.946	0.949	0.896	0.948	0.696	0.720
8.000	1.022	0.867	0.865	0.955	1.096	0.905	0.971	0.971	0.925	0.958	0.809	0.818
10.000	1.019	0.869	0.870	0.954	1.089	0.907	0.968	0.968	0.929	0.958	0.810	0.829
		Blood				Extrathoracic region				Gall bladder		
0.015	0.002	–	–	–	0.042	–	–	0.012	0.004	–	–	–
0.030	0.179	0.095	0.059	0.096	0.507	0.020	0.222	0.240	0.418	0.034	0.199	0.024
0.040	0.542	0.361	0.223	0.325	0.893	0.116	0.500	0.520	0.886	0.181	0.531	0.101
0.050	0.912	0.670	0.411	0.564	1.206	0.257	0.761	0.778	1.260	0.381	0.813	0.198
0.080	1.291	1.074	0.656	0.847	1.488	0.501	1.058	1.076	1.630	0.699	1.132	0.370
0.200	1.013	0.894	0.627	0.745	1.253	0.552	1.000	1.009	1.246	0.691	0.963	0.405
0.400	0.914	0.832	0.655	0.749	1.137	0.603	0.969	0.983	1.117	0.701	0.924	0.471
0.600	0.898	0.828	0.693	0.772	1.099	0.650	0.970	0.977	1.070	0.711	0.923	0.507
0.800	0.895	0.836	0.727	0.796	1.080	0.674	0.975	0.980	1.053	0.730	0.924	0.556
2.000	0.913	0.872	0.823	0.865	1.052	0.781	0.989	0.991	1.014	0.809	0.949	0.697
8.000	0.941	0.914	0.899	0.924	1.029	0.870	0.994	0.995	1.001	0.881	0.953	0.801
10.000	0.942	0.917	0.902	0.926	1.025	0.872	0.992	0.992	0.996	0.880	0.947	0.805
		Heart				Kidneys				Muscle		
0.015	0.001	–	–	–	–	0.002	–	–	0.036	0.038	0.018	0.018
0.030	0.247	0.052	0.065	0.137	0.080	0.370	0.039	0.057	0.393	0.492	0.208	0.203
0.040	0.697	0.232	0.235	0.402	0.305	0.856	0.147	0.203	0.693	0.845	0.375	0.367
0.050	1.119	0.461	0.423	0.663	0.557	1.256	0.279	0.361	0.938	1.112	0.517	0.506
0.080	1.506	0.791	0.669	0.947	0.886	1.611	0.468	0.568	1.164	1.323	0.659	0.648
0.200	1.168	0.720	0.652	0.831	0.768	1.252	0.426	0.500	1.002	1.101	0.603	0.593
0.400	1.033	0.711	0.683	0.815	0.741	1.110	0.442	0.508	0.951	1.020	0.610	0.602
0.600	0.999	0.730	0.717	0.827	0.757	1.059	0.469	0.529	0.942	0.998	0.631	0.624
0.800	0.989	0.747	0.749	0.841	0.769	1.042	0.497	0.557	0.944	0.993	0.654	0.648
2.000	0.978	0.818	0.841	0.891	0.837	1.015	0.620	0.670	0.960	0.992	0.743	0.739
8.000	0.980	0.880	0.902	0.930	0.895	0.999	0.759	0.798	0.971	0.991	0.842	0.840
10.000	0.978	0.883	0.902	0.931	0.896	0.996	0.770	0.804	0.969	0.989	0.849	0.846
		Oral mucosa				Pancreas				Prostate		
0.015	0.073	–	0.015	0.017	0.002	–	–	–	–	–	–	–
0.030	0.517	0.019	0.282	0.294	0.353	0.033	0.034	0.080	0.141	0.198	0.008	0.010
0.040	0.842	0.103	0.546	0.559	0.812	0.191	0.158	0.282	0.500	0.531	0.065	0.070
0.050	1.106	0.231	0.789	0.800	1.211	0.418	0.315	0.501	0.870	0.851	0.165	0.184
0.080	1.394	0.458	1.075	1.089	1.588	0.801	0.552	0.778	1.225	1.211	0.364	0.379
0.200	1.219	0.526	1.029	1.037	1.238	0.736	0.538	0.697	1.053	1.002	0.382	0.421
0.400	1.111	0.587	1.005	0.992	1.103	0.729	0.557	0.708	0.935	0.951	0.445	0.467
0.600	1.080	0.635	0.988	0.989	1.065	0.740	0.591	0.728	0.938	0.921	0.461	0.507
0.800	1.059	0.671	0.990	0.990	1.045	0.758	0.630	0.755	0.940	0.938	0.488	0.539
2.000	1.032	0.768	0.994	0.988	1.021	0.823	0.744	0.837	0.950	0.930	0.642	0.667
8.000	0.997	0.835	0.974	0.973	1.002	0.878	0.841	0.893	0.944	0.921	0.787	0.814
10.000	0.992	0.836	0.968	0.966	0.998	0.879	0.842	0.893	0.943	0.919	0.800	0.818

Table 2. (Continued.)

Energy (MeV)	AP	PA	RLAT	LLAT	AP	PA	RLAT	LLAT	AP	PA	RLAT	LLAT
		Small intestine				Spleen				Thymus		
0.015	0.025	–	0.001	0.001	0.001	–	–	0.001	0.002	–	–	–
0.030	0.612	0.028	0.112	0.108	0.262	0.134	0.005	0.382	0.396	0.019	0.051	0.085
0.040	1.111	0.163	0.299	0.286	0.670	0.438	0.039	0.853	0.918	0.121	0.212	0.292
0.050	1.483	0.364	0.480	0.460	1.027	0.747	0.100	1.233	1.326	0.285	0.381	0.503
0.080	1.754	0.699	0.699	0.670	1.323	1.108	0.224	1.503	1.691	0.552	0.619	0.774
0.200	1.336	0.680	0.666	0.639	1.029	0.920	0.249	1.172	1.334	0.552	0.631	0.743
0.400	1.171	0.688	0.685	0.670	0.936	0.863	0.304	1.065	1.181	0.559	0.661	0.750
0.600	1.113	0.710	0.714	0.701	0.924	0.851	0.353	1.044	1.117	0.594	0.699	0.783
0.800	1.089	0.734	0.742	0.728	0.918	0.858	0.398	1.035	1.091	0.619	0.730	0.802
2.000	1.045	0.808	0.828	0.817	0.940	0.893	0.567	1.028	1.047	0.716	0.821	0.868
8.000	1.016	0.870	0.891	0.886	0.950	0.918	0.740	1.014	1.016	0.817	0.887	0.918
10.000	1.012	0.873	0.893	0.889	0.949	0.918	0.751	1.011	1.011	0.826	0.890	0.921

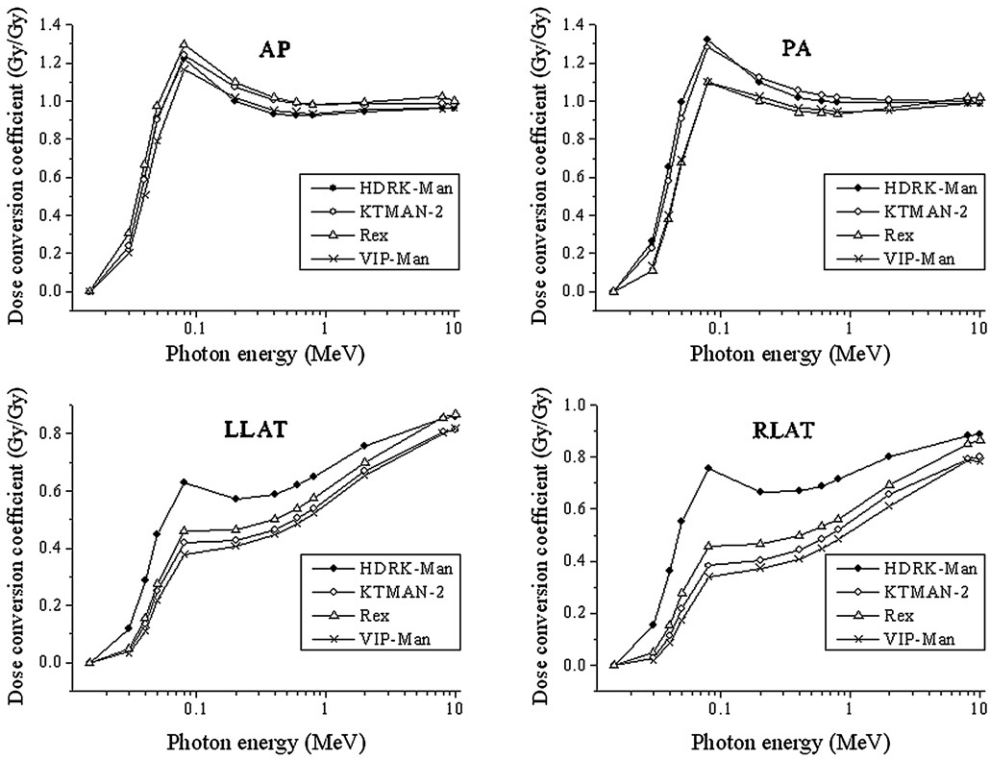

Figure 4. Dose conversion coefficients for lung calculated by HDRK-Man, KTMAN-2, Rex and VIP-Man.

For a quantitative comparison of the dose conversion coefficients from HDRK-Man with those from the other voxel models, this study defined 'percent dose deviation (δ)'. The percent dose deviation, which shows the extent to which a dose conversion coefficient or simply an

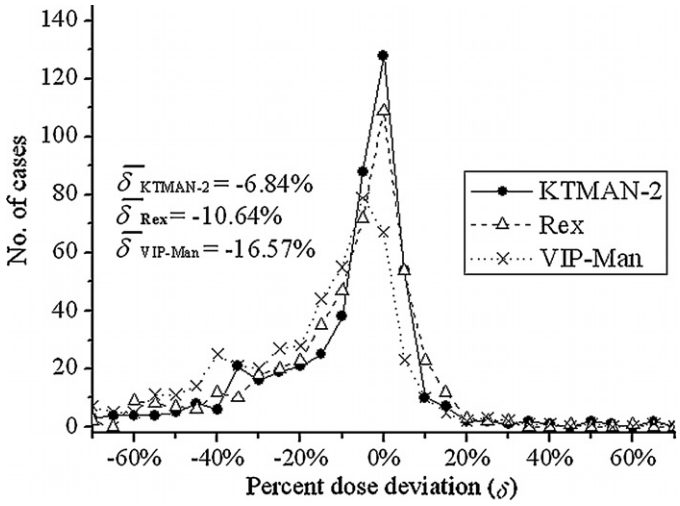

Figure 5. Distribution of percent dose deviations (δ) calculated between three reference voxel models and HDRK-Man.

organ dose calculated by a voxel model deviates from the value calculated from HDRK-Man, is defined as follows for a voxel model, M:

$$\delta = \frac{D_M - D_{\text{HDRK-Man}}}{D_{\text{HDRK-Man}}} \times 100\% \tag{2}$$

where D_M and $D_{\text{HDRK-Man}}$ are the dose conversion coefficients calculated from voxel model M and HDRK-Man, respectively, under identical irradiation conditions. A positive value of δ means that the voxel model M yields a higher dose conversion coefficient than HDRK-Man for a given condition; likewise, a negative value indicates a lower value.

Figure 5 shows the distribution of δ for KTMAN-2, Rex and VIP-Man, for a total of 44 irradiation conditions and 11 organs (i.e. $44 \times 11 = 484$ cases)—that is, 4 irradiation geometries (AP, PA, RLAT and LLAT), 11 photon energies (0.03, 0.04, 0.05, 0.08, 0.2, 0.4, 0.6, 0.8, 2, 8 and 10 MeV) and 11 major organs and tissues (i.e. gonads, red bone-marrow, colon, lung, stomach, bladder, liver, esophagus, thyroid, skin and bone surface) for which the organ dose values are available for all of the voxel models considered in the present study.

The results show that KTMAN-2, Rex and VIP-Man tend to yield lower dose conversion coefficients than HDRK-Man, which is reasonable considering that HDRK-Man is smaller than the other models, especially in the torso, resulting in less shielding for the internal organs. The average ($\bar{\delta}$) of the percent dose deviations was calculated as -7%, -11%, and -17% for KTMAN-2, Rex and VIP-Man, respectively. The largest deviation was observed for VIP-Man, which is significantly heavier than HDRK-Man. Even though KTMAN-2 and HDRK-Man have similar heights and weights, KTMAN-2 tends to yield somewhat lower values than HDRK-Man, due to the facts that (1) HDRK-Man has a smaller torso than KTMAN-2 and (2) the arms of HDRK-Man are shifted backward, meaning that the internal organs positioned mainly in the torso region are less shielded from radiation in RLAT and LLAT geometries. Nevertheless, KTMAN-2 showed the best agreement with HDRK-Man, which was expected, as they have similar heights and weights. The discrepancy of the dose conversion coefficients between these two models was less than 20% for 75% of a total of 484 irradiation cases. The discrepancy exceeded 50% for only 6% of the total cases.

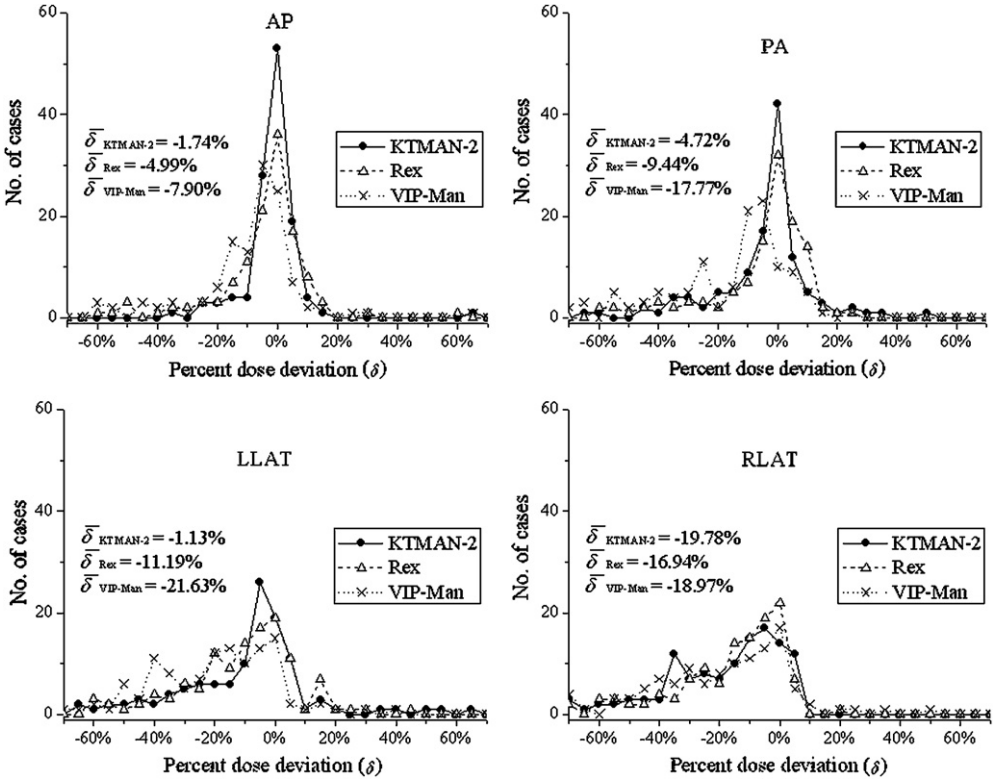

Figure 6. Distribution of percent dose deviations (δ) for AP, PA, LLAT and RLAT geometries.

Figure 6 shows the distributions of δ values for each of AP, PA, RLAT and LLAT geometries, separately. The results generally show that the discrepancies of dose conversion coefficients between HDRK-Man and the other models are the least significant for AP geometry, which is mainly because the most organs are located anterior in the body and less shielded for the radiations from the front side. The results also clearly show that, for RLAT and LLAT geometries, KTMAN-2, Rex and VIP-Man tend to give lower dose conversion coefficients than HDRK-Man, which is again due to the fact that HDRK-Man has a relatively smaller trunk and the arms are shifted backward, resulting in less shielding effect.

4. Conclusions

In the present study, a Korean adult male voxel model, called HDRK-Man, was constructed using high-resolution color photographic slice images of a Korean adult male cadaver. The model dimensions, including the body height and weight, the skeletal mass, and the dimensions of the individual organs, were matched to the reference Korean data. The resulting model was then implemented into MCNPX to calculate the dose conversion coefficients, which were found to be reasonable when compared with the values from the other adult voxel models. HDRK-Man, which is 171 cm in height and 68 kg in weight and has organs and tissues of reference Korean size, is believed to adequately represent the average Korean workers and thus can be used for more accurate calculation of dose conversion coefficients for the Korean

workers in the future. It should be emphasized, however, that the current version of HDRK-Man, with its reference Korean-adjusted dimensions, was developed for radiation protection purposes only and therefore cannot be used in medical applications for which patient-specific representations of a human body are necessary.

Acknowledgments

This work was supported by the Korean Ministry of Education, Science and Technology through the Korea Institute of Nuclear Safety (KINS), ERC (RII-2000-067-03002-0) and BAERI (M20508050003-05B0805-00310).

References

Caon M 2004 Voxel-based computational models of real human anatomy: a review *Radiat. Environ. Biophys.* **42** 229–35

Chao T C 2001 The development and application of a tomographic whole-body model for Monte Carlo organ dose calculation*PhD Dissertation* Department of Nuclear Engineering and Science Rensselaer Polytechnic Institute, Troy, NY, USA

Chung M S, Kim J Y, Hwang W S and Park J S 2002 Visible Korean human: another trial for making serially sectioned images *Proc. SPIE* **4681** 171–83

Dimbylow P J 1996 The development of realistic voxel phantoms for electromagnetic field dosimetry *Proc. Int. Workshop on Voxel Phantom Development* (Chilton: National Radiological Protection Board) pp 1–7

Gibbs S J, Pujol A, Chen T-S, Malcolm A W and James A E 1984 Patient risk from interproximal radiography *Oral Surg. Oral Med. Oral Pathol.* **58** 347–54

IAEA 1998 Compilation of anatomical, physiological and metabolic characteristics for a reference Asian Man *IAEA-TECDOC-1005, International Atomic Energy Agency, Vienna, Austria*

ICRP 1975 Reference Man: Anatomical, Physiological and Metabolic Characteristics *ICRP Publication 23* (Oxford: Pergamon)

ICRP 1994 Basic Anatomical and Physiological Data for Use in Radiological Protection: the Skeleton *ICRP Publication 70* (Oxford: Pergamon)

ICRP 2002 Basic Anatomical and Physiological Data for Use in Radiological Protection: Reference Values *ICRP Publication 89* (Oxford: Pergamon)

ICRU 1992 Photon, Electron, Proton and Neutron Interaction Data for Body Tissues *ICRU Report No 46* (Bethesda, MD: International Commission on Radiation Units and Measurement)

Kramer R, Vieira J W, Khoury H J, Lima F R A and Fuelle D 2003 All about MAX: a male adult voxel phantom for Monte Carlo calculations in radiation protection dosimetry *Phys. Med. Biol.* **48** 1239–62

Lee C and Lee J 2006 Computational anthropomorphic phantoms for radiation protection dosimetry: evolution and prospects *Nucl. Eng. Technol.* **38** 239–50

Lee J K and Kim H K 2004 Formulation of the reference Korean for radiation protection *iTRS/TR-2004-01, Ministry of Science and Technology, Seoul, Korea*

Park J S, Chung M S, Hwang S B, Shin B and Park H S 2006a Visible Korean human: its techniques and applications *Clin. Anat.* **19** 216–24

Park S, Lee J K, Kim J I, Lee Y J, Lim Y K, Kim C S and Lee C 2006b *In vivo* organ mass of Korean adults obtained from whole-body magnetic resonance data *Radiat. Prot. Dosim.* **118** 275–9

Pelowitz D B 2005 MCNPX user's manual version 2.5.0 LA-CP-05-0369, Los Alamos National Laboratory, Los Alamos, USA

Saito K, Wittmann A, Koga S, Ida Y, Kamei T, Funabiki J and Zankl M 2001 Construction of a computed tomographic phantom for a Japanese male adult and dose calculation system *Radiat. Environ. Biophys.* **40** 69–76

Schlattl H, Zankl M and Petoussi-Henss N 2007 Organ dose conversion coefficients for voxel models of the reference male and female from idealized photon exposures *Phys. Med. Biol.* **52** 2123–45

Tanaka G, Nakahara Y and Nakazima Y 1989 Japanese reference man 1988-IV Studies on the weight and size of internal organs of normal Japanese *Nippon Igaku Hoshasen Gakkai Zasshi* **49** 344–64

Xu X G, Chao T C and Bozkurt A 2000 VIP-Man: an image-based whole-body adult male model constructed from color photographs of the visible human project for multi-particle Monte Carlo calculations *Health Phys.* **78** 476–86

Zankl M, Becker J, Fill U, Petoussi-Henss N and Eckerman K F 2005 GSF male and female adult voxel models representing ICRP Reference Man—the present status *Proc. The Monte Carlo Method: Versatility Unbounded in a Dynamic Computing World (Chattanooga, TN: American Nuclear Society)*

Zubal I G, Harrell C R, Smith E O, Rattner Z, Gindi G and Hoffer P B 1994 Computerized three-dimensional segmented human anatomy *Med. Phys.* **21** 299–302